# Magnetic Field Imaging by Differential Equations

Hisashi ENDO Seiji HAYANO Yoshifuru SAITO
Department of Electrical and Electronic Engineering, Hosei University

Tosiyasu L.KUNII
Computational Science Research Centre, Hosei University

A novel methodology is proposed to visualize the electromagnetic vector fields. First, in order to apply the field theory of computer graphics proposed in this paper, an electromagnetic field vector is represented as a color image. According to our theory, the high-resolution image can be generated in accordance with like a natural phenomenon. Consequently, it is possible to obtain more precise electromagnetic field from the poor measured data. Secondary, we have applied our method to the practically experimented magnetic fields. As a result, validity of our method has been verified.

## 1. Introduction

Modern electromagnetic compatibility engineering requires a lot of electromagnetic field data for design of the electric as well as electronic devices utilizing high frequency semiconductors [1,2]. The electromagnetic field data visualizing the precise space distributing characteristics are essentially enormous data quantity, because the electromagnetic fields spread into a space around the electronic devices with infinitely high-resolution. In order to handle to such the electromagnetic field data efficiently, two approaches may be considered. One is the inverse solution approach, which recovers the electromagnetic fields from its electromagnetic field source evaluated as a solution of inverse problem. The other is to employ a digital image handling technique.

In the present paper, we propose an electromagnetic data imaging by means of the differential equations. This method makes it possible to recover the electromagnetic fields with any resolution as a solution of the partial differential equations.

## 2. Visualization of Electromagnetic Fields

### 2.1 Vector Field Imaging

Any vector fields can be represented in terms of the three orthogonal components. This fact leads to a color graphics visualizing methodology for the vector fields. Namely, the $x$, $y$ and $z$ components of vector fields in Cartesian coordinate system are projected onto the *red*, *green* and *blue* components of color image, respectively. For example, the projection of the magnetic field vector components shown in Figs. 1(a)-(c) to the red, green and blue components of color image visualizes a vector distribution shown in Fig. 1(d) in terms of the color image as shown in Fig. 1(e). Conversely, the color image in Fig. 1(e) can be represented by the vector distribution in Fig. 1(d).

### 2.2 Image Governing Equation and Its solution

Image governing equation of the static images is a Poisson's equation [3]:

$$-\nabla^2 U_{color} = \sigma_{color}, \qquad color = Red, Green, Blue, \quad (1)$$

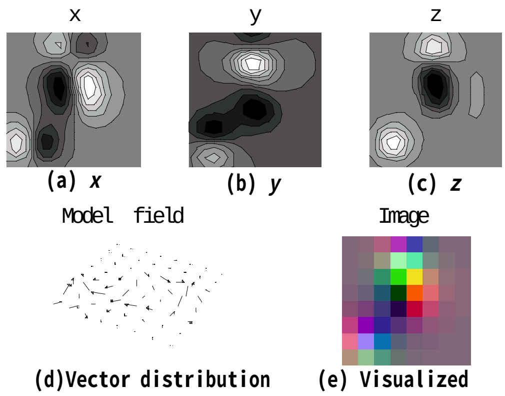


**Fig.1。 Vector field imaging**
**(a)-(c) vector components, (d) vector distribution and (e) visualized image**

where $U_{color}$ and $\sigma_{color}$ are the scalar potentials and source densities, respectively. The subscripts *color* denotes each of the color components. Because of the scalar potential $U$ in Eq. (1) corresponding to the image data, Laplacian operator removes the constant and first spacial derivative terms from the image data. This means that the color image data can be compressed without losing any information when solving Eq. (1) exactly. Practical Laplacian operator is replaced by the relevant finite differences. In this paper, we employ a nine-point formula [4]:

$$\nabla^2 U = \frac{\partial^2 U}{\partial x^2} + \frac{\partial^2 U}{\partial y^2} \approx \frac{1}{6}\begin{bmatrix} U_{i+1,j+1} + U_{i+1,j-1} + U_{i-1,j+1} + U_{i-1,j-1} \\ +4\left(U_{i+1,j} + U_{i-1,j} + U_{i,j+1} + U_{i,j-1}\right) \\ -20U_{i,j} \end{bmatrix}, \quad (2)$$

where the step-widths in the direction of $x$- and $y$- axes have been assumed to be 1. Also, zero Dirichlet boundary condition has been assumed at the edges of graphics screen. The image source densities $\sigma_{color}$, *color* = *Red*, *Green*, *Blue*, by applying Eq. (2) to each of the vector components shown in Figs.1 (a)-(c) are shown in Figs. 2(a)-(c).

Several numerical methods can be available to solve for the image governing equation (1). When it is required an approximate image recovery, the finite element method whose meshes become one of the best wire-frame representations of the image source densities is a preferable numerical scheme. However, if it is required an exact recovery of original image, then it is essential to use the same nodal or pixel layout to Figs. 1(a)-(c). This means that we have to solve Eq. (1) using the regular equi-spaced mesh system [5]. Thereby, we have applied a conventional finite difference scheme (2) to Eq. (1). Fig. 3 shows the recovered magnetic field vectors and its color image. A correlation analysis between the images in Fig. 3(b) and Fig. 1(e) reveals that the vector distribution as well as visualized image in Fig. 3 are exactly same ones as that of Fig. 1.

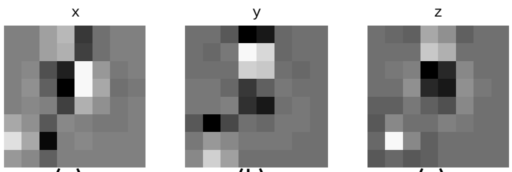

(a) *x* (b) *y* (c) *z*

**Fig. 2 Image source densities**

(a) Recovered vector field (b) Visualized

**Fig.3 Recovered vector field (8x8pixels)**

### 2.3 High-resolution Vector Field Generation

The image governing equation (1) is a typical Poisson type partial differential equation so that its solution is capable of representing the image and vector distribution with any resolutions. When the source densities are given in terms of the analytical functions, then it is possible to synthesis an exact image with any resolutions as a solution of the Poisson's equation. However, the image source densities in Eq. (2) are always given in terms of the numerical values. This is a fundamental difference between the classical and modern image Poisson's equations, and also leads to synthesis with finite accuracy determined by the discretization accuracy of the source densities in Eq. (1). As shown in Fig. 4(a), an exact image is recovered when solving Eq. (1) with the original image pixel layout, and an approximate image synthesis is carried out when solving Eq. (1) with a different pixel layout. Fig. 4(b) shows the synthesized vector distribution and its color-visualized image with 4-th times larger resolution than those of Fig. 1. A correlation coefficient between Fig. 4(a) and Fig. 4(b) is 0.93, which means a fairly good recoverability.

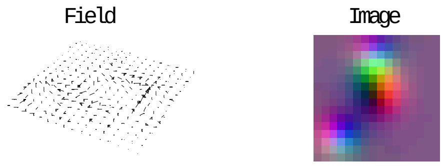

(a) Exact

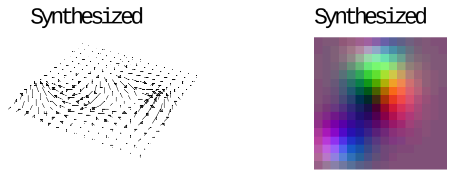

(b) Generated from Fig.1 (e)

**Fig.4 High-resolution vector field generation (16x16 pixels)**

## 3.Experimental Verification in Magnetic Fields

### 3.1 DC/DC Converter with Film-type Transformer

An experiment is carried out in order to verify our approach. We have measured the magnetic field distributing over the DC/DC converter shown in Fig.5(a)[2]. Figure 5(b) is the visualized magnetic field image when the output voltage of sensor coil locating at the center of film-type transformer takes a maximum in value. Each of the orthogonal magnetic field components is measured by changing direction of the solenoidal sensor coil. Since the number of measured points is 32x32, then the visualized magnetic field image shown in Fig. 5(b) has 32x32 resolution.

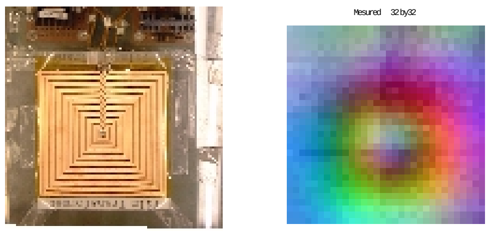
(a) DC/DC converter (b) Magnetic field imaging

**Fig. 5 DC/DC converter using film-type transformer**

### 3.2 Estimation of Magnetic Field Distribution

According to the field theory of computer graphics, the solution of image governing equation (1) yields the vector field images with any resolutions in accordance with like a natural phenomenon. Namely, the vector fields are represented in term of the exponential functions. Figure 6 shows the low-resolution color images obtained by regularly sampling the pixels in Fig. 5(b). By applying the image governing equation to these poor images, it is possible to obtain the high-resolution magnetic field images. Figures 7(a), (b) and (c) are the 32x32 resolution images generated from the low-resolution magnetic field images in Figs. 6(a), (b) and (c), respectively. The correlation coefficients between Fig. 5(b) and Figs. 7(a)-(c) become 0.91, 0.80 and 0.50, respectively. The reason why we can obtain the good estimations by solving Eq. (1) with the low-resolution source densities is that the finite difference method employed here to solve Eq. (1) gives a solution with smaller truncation error when applying a large number of nodal points or pixels. Thus, it is obvious that the image Poisson equation (1) has a versatile possibility to handle the computer graphics as well as visualized vector fields.

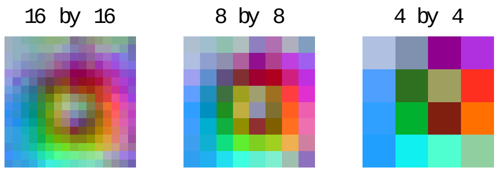


(a) (b) (c)

**Fig. 6 Low-resolution magnetic fields (a)16x16, (b) 8x8 and (c) 4x4 resolutions**

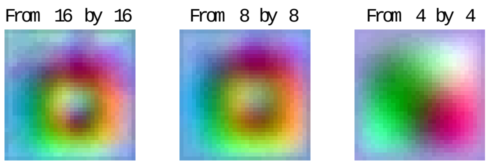


(a) (b) (c)

**Fig. 7 Generated high-resolution magnetic field distributions (a) 16x16 to 32x32, (b) 8x8to 32x32 and (c) 4x4 to 32x32 resolutions**

## 4. Conclusions

We have proposed a new vector field visualization method based on the field theory of computer graphics, which makes it possible to apply the classical field theory to represent the computer color graphics. More precisely, the orthogonal vector components have been projected onto the red, green and blue components of the color image. This projection has visualized the vector fields in terms of the color computer graphics. Applying the Laplacian operator to the visualized vectors has yielded the image source densities of the vector fields, and also the solutions using these image source densities have generated the high-resolution vector fields with good accuracy even if they are the practically measured field distributions.

## References


[1] S.Hayano, H.Saotome, Y.Nakajima and Y.Saito, “A new type high frequency transformer”, *IEEE* Transaction on Magnetics、Vol.MAG-27, No.6, Nov. 1991, pp.5205-5207.

[2] T.Ogawa, H.Saotome, S.Hayano and Y.Saito, "Realization of a coreless transformer and its application to a DC/DC converter," Elektrotechn.CAS., 44(1993), No.7, pp.238-241.

[3] H.Endo, S.Hayano, Y.Saito, M.Sakuma, K.Horii, “An Analysis of Electromagnetic Field Distribution By Means of Image Processing”, Magnetic Society of IEEJ, MAG-99-141, 1999.

[4] T. Akasaka, “Numerical Calculations”, Corona (1968).

[5] W.H.Press, B.P.Flannery, S.A.Teukolsky and W.T.Vetterling, “Numerical Recipes in C”, Cambridge University Press (1988).

[6] P.P.Silvester and R.L.Ferrari, "Finite elements for elements for electrical engineers", Cambridge University Press (1983)

**Keywords.**

Image Processing, Electromagnetic Field Analysis, Finite Difference Method, Finite Element Method, DC/DC Converter

---

**Summary.**

# 微分方程式による磁界分布の可視化

遠藤 久　　早野誠治　　齋藤兆古
法政大学工学部電気電子工学科

國井利泰
法政大学計算科学研究センター

本論文では、画像処理の一方法とそれを応用した電磁界ベクトルフィールドの可視化方法を提案する。第１に、本論文で提案する画像処理方法を電磁界分布解析へ応用するために、３次元ベクトルフィールドをカラー画像で表現する。そこで得られる画像を偏微分方程式で記述し、その方程式を解くことであらゆる画素数の画像を生成する。結果として、測定点数の少ないデータからより詳細な電磁界分布データが得られる。第２に、検証実験として、高周波駆動を前提とするフィルム状変圧器を用いた DC/DC コンバータ周辺に分布する磁界を測定し、本手法を適応する。

**キーワード.**

画像処理、電磁界分布解析、有限差分法、有限要素法、DC/DC コンバータ、